ACS SyntheticBiology

Research Article

pubs.acs.org/synthbio

Photoswitch Nucleic Acid Catalytic Activity by Regulating Topological Structure with a Universal Supraphotoswitch

Xingguo Liang,*[,†,‡] Mengguang Zhou,[†] Kenjiro Kato,[†] and Hiroyuki Asanuma*[,†]

[†]Graduate School of Engineering, Nagoya University, Furo-cho, Chikusa, Nagoya, 464-8603, Japan

[‡]College of Food Science and Engineering, Ocean University of China, Qingdao 266003, China

Supporting Information

ABSTRACT: We demonstrated the generality of a strategy for photoswitching the activity of functional oligonucleotides by modulating their topological structure. Our strategy was proved to be versatile because it can be used to photoregulate functional oligonucleotides, e.g., ribozymes and DNAzymes, which have two binding arms and a catalytic loop. Repeated reversible photoregulation of RNA cleavage by a ribozyme or a DNAzyme was achieved by attaching two photoresponsive strands, artificial oligomers involving azobenzene moieties and nucleobases capable of forming a duplex as the supraphotoswitch. Individual strands were attached to the 3′ and 5′ ends of a RNA-cleavage oligonucleotide. Thus, the topological structure of the ribozyme or DNAzyme was constrained, and RNA cleavage was greatly suppressed when the supraphotoswitch duplex formed (OFF state). In contrast, RNA cleavage resumed when the supraphotoswitch duplex dissociated (ON state). Light irradiation was used to repeatedly switch the supraphotoswitch between the ON and OFF states so that RNA cleavage activity could be efficiently photoregulated. Analysis of the regulatory mechanism showed that topological constraints suppressed the RNA cleavage by causing both structural changes at the catalytic site and lower binding affinity between the RNA substrates and the functional oligonucleotides.

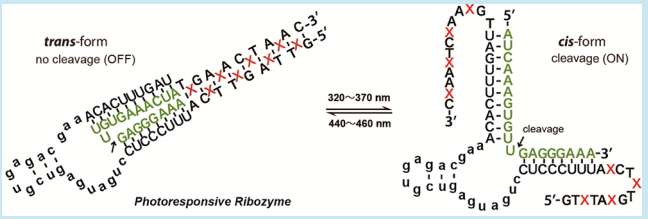

KEYWORDS: *photoswitch, RNA cleavage, topological structure, azobenzene, modified nucleic acid*

Photoregulation of biological molecules is a robust tool used to investigate the mechanisms of their biological functions.[1−5] On−off switching of a biological function with light irradiation is a facile method for selectively manipulating a biologically active molecule. When light is used to manipulate spatiotemporally the activity of a biological process in living cells, secondary and unintentional perturbations of cellular processes can be minimized.[6−10] Quantitative laser-initiated photoregulation of biological activities is widely used for research in cell and developmental biology.[1] Moreover, *in vivo* applications of photoactive systems might facilitate the development of new therapies that use photoresponsive molecules.[11]

Chemical modifications and genetic engineering have been used to construct photoresponsive biological systems.[12−14] An effective chemical approach is to covalently attach a photoresponsive compound to the target biological molecule.[1−13] For example, many kinds of photoresponsive systems use photocaged nucleic acids, proteins, or other types of molecules.[15−21] The biological activity of these molecules can be switched on after the attached photoresponsive groups are removed. However, the biofunction cannot be switched off again, and the released caging moieties might have cytotoxic effects. Alternatively, repeatable reversible photoregulation can be achieved by covalently modifying the target bioactive molecule with a compound that reversibly photoisomerizes between two conformations (isomers) upon irradiation with specific wavelengths of light.[22−28] However, in many examples of reversible photoregulation, the effects of photoresponsive groups on the biological activity of the modified target biomolecule are variable, and clear-cut photoregulation usually requires advanced molecular design. In some cases, optimal positioning of chemical modifications that mediate efficient photoregulation is found by extensive experimentation and trial and error.[27] Moreover, findings from these studies are not necessarily relevant when designing a new photoresponsive system targeting a different biomolecule. Facile, widely applicable methods for the construction of reversible photoswitches for biological molecules should be developed.

Previously, to design a light-driven DNA nanomachine that operated at the single-molecule level, we constructed a photoresponsive hairpin-like 10−23 DNAzyme, and the RNA digestion activity of molecule was efficiently photoregulated.[28] A DNA-based supraphotoswitch capable of reversibly forming a noncovalent duplex was covalently attached to the DNAzyme, and the formation and dissociation of the duplex could be simply regulated by irradiation with different wavelengths of light.[29−32] We hypothesized that hairpin-like structure formed by visible-light irradiation (*trans*-form) prevented formation of active conformation of DNAzyme because of the topological constraint, whereas UV light irradiation (*cis*-form) unlocked the

Received: November 11, 2012
Published: February 13, 2013

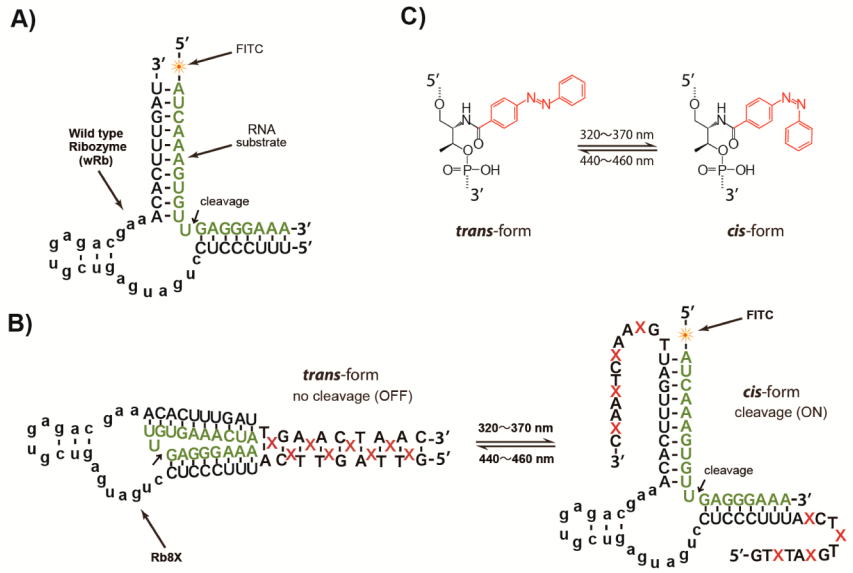

Figure 1. Molecular design of a photoresponsive hammerhead ribozyme (Rb8X) bearing azobenzene residues (X, in red). (A) The wild-type ribozyme/substrate complex. (B) Reversible changes are induced in the secondary structures Rb8X/substrate complex with light irradiation. Upon irradiation with visible light (440−460 nm), the two strands of the supraphotoswitch hybridize with each other to form a stable duplex, and the steric hindrance caused by the proximity of the arms limited the topological structure of the catalytic loop. Upon irradiation with UV light (320−370 nm), the duplex dissociates, and the topological constraint is released. In (A) and (B), the catalytic loop is shown using lower-case letters, and the RNA substrate (in green), the sequence of a part of c-erbB-2 mRNA, is labeled with a fluorophore (FITC, Fluorescein isothiocianate) at the 5′ end. (C) Structure of the azobenzene residue and its photoisomerization.

constrained conformation by the dissociation of stem region. However, we did not unambiguously prove that the photoregulation has been realized as we designed. We found that a stable secondary structure could form between two arms of 10−23 DNAzyme we used. One possibility is that not the topological structure change itself, but the difficult binding of RNA substrate to two arms of 10−23 DNAzyme caused the big difference in activity between *trans* and *cis* form. It is significant to study the mechanism and generality of this strategy for optimizing molecular design of photoresponsive functional nucleic acids and understanding the mechanism of corresponding functional nucleic acids. Here, we propose to use photoswitching of topological conformation as a general approach for photoregulating the activity of functional nucleic acids (ribozymes and DNAzymes) that bind to their target DNA or RNA substrate with two arms. The molecular design is simple, the modified DNAs are attached to the 5′ and 3′ ends of the functional nucleic acid, and the detailed structure of catalytic sequence is almost irrelevant to photoregulation. Reversible photoregulation of the hammerhead ribozyme and 8−17 DNAyzme, two RNA cleavage catalysts, was achieved using this strategy. The mechanism of regulation of RNA cleavage was also investigated, and we found that topological constraint greatly affected the RNA cleavage activity. The secondary structure formed between two arms was also favorable for improving the photoregulation efficiency.

RESULTS AND DISCUSSION

Chemical modifications are usually done at the functional site of target biomolecules to take effect. However, these modifications can affect the bioactivity or the binding of some enzymes we do not expect. In this study, we tried to clarify a new strategy of chemical modification of nucleic acids by pulling together their two ends to suppress their function due to the topological structure change. More interestingly, the recovery of their function was realized by removing the constraint. We used azobenzene-modified oligonucleotides for photoregulation, and it can be expanded to other chemical modifications and other biomolecules. The approach of regulating biological functions by changing high-dimentional structure of biomolecules was explored.

Photoregulation of RNA Digestion by Modulating the Topology of a Hammerhead Ribozyme. *Molecular Design of Photoresponsive Ribozyme with a Controllable Topological Structure.* Previously, we designed a light-driven, machine-like 10−23 DNAzyme that catalyzes the digestion of RNA and has a topological conformation that can be photoregulated to switch on and off the catalytic activity.[28] The two ends of the modified DNAzyme formed a 9 bp duplex with 7 azobenzenes, which had the same sequences as reported in a model system.[29] However, the generality of this molecular design was unclear. Also only GU and AU site can be cleaved efficiently by 10−23 DNAzyme, and a new design is required for other cleavage sites. Here, we engineered a ribozyme with an azobenzene-modified DNA oligonucleotide covalently linked to each end (5′ and 3′) of the ribozyme (Figure 1). The hammerhead ribozyme was selected as the model system because of its relatively small size, inherent simplicity, and well-defined tertiary structure. In the native conformation, the hammerhead ribozyme is a single-stranded RNA that self-cleaves.[33,34] It can also be modified to include a conservative catalytic core and two binding arms; together, these modifications confer site-specific RNA cleavage activity to the hammerhead ribozyme.[34] Modified hammerhead ribozymes are

dx.doi.org/10.1021/sb300120n | *ACS Synth. Biol.* 2013, 2, 194−202

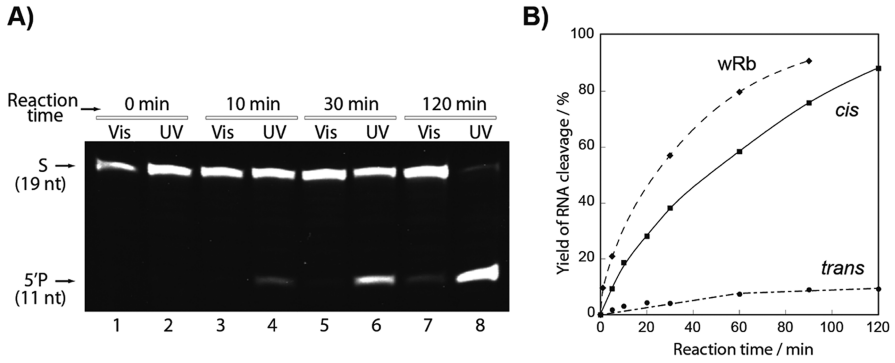

Figure 2. Time course of RNA cleavage by hammerhead ribozymes under multiturnover conditions. (A) Gel analysis of cleavage reaction. Lane 1, 3, 5, 7: RNA cleavage after Rb8X was irradiated for 1 min with visible light (Vis); Lane 2, 4, 6, 8: RNA cleavage after Rb8X was irradiated for 5 min with UV light. (B) Time course profile of *trans*-Rb8X (circles, dash-dotted line), *cis*-Rb8X (squares, solid line), and wRb (diamonds, dashed line). Conditions: 0.1 μM ribozyme, 1.0 μM sRb (RNA substrate), 1.0 M NaCl, 10 mM $MgCl_2$, 37 °C.

promising as therapeutic agents in treatments for amyotrophic lateral sclerosis (ALS) or AIDS.[35,36] The three-dimensional structure of a full-length hammerhead ribozyme shows that the 5′ and 3′ ends are separated in space.[37] We expected that pulling the 5′ and 3′ ends together would cause a substantial decrease of its catalytic activity.

A hammerhead ribozyme sequence was designed to catalyze the cleavage ErbB-2 (human epidermal growth factor receptor 2) mRNA (Figure 1A). ErbB-2 is overexpressed in breast cancers, ovarian cancers, and stomach cancers.[38−40] Supraphotoswitch strands, each with 4 azobenzenes and 9 bases, were attached to the 5′ and 3′ ends of the ribozyme (Figure 1B). For reactions at lower ion strength (lower T_m), 8 azobenzenes were used instead of previous 7 ones.[28] Longer sequence and more azobenzenes can form more stable duplex for *trans* form so that the cleavage was suppressed more efficiently. On the other hand, dissociation after UV light irradiation (*cis* form) becomes less.[13,29] For reaction under physiological conditions, 8−10 base pairs and 7−9 azobenzens are appropriate.

When azobenzene residues (Xs) take *trans* form with a planar structure, an artificial duplex can form between the strands of the supraphotoswitch, and the 5′ and 3′ ends as well as the arms of ribozyme are then pulled together. The lengths of two arms were designed to be different so that the conformation of substrate at the cleavage site changed more than the asymmetric design having two arms with the same length, when the supraphotoswitch formed the duplex and the two arms of the catalyst were pulled together (Figure 1A). The added topological constraint should block the RNA cleavage. In contrast, when azobenzene residues take the nonplanar *cis* form, the two strands of the supraphotoswitch duplex should separate, and the cleavage activity should be recovered because the topological constraint is released. Irradiation with visible light (440−460 nm) can induce the azobenzenes to take the *trans* form, while UV light (320−370 nm) induces them to take the *cis* form. It should be noted that for "*trans* form" we describe in this study, more than 90% of azobenzenes are in *trans* form. For "*cis* form", however, only about 40−50% of azobenzenes are in *cis* form actually.[29−31]

Cleavage Reactivity Changes with Light Irradiation. Ribozyme Rb8X activity, sequence-specific cleavage of the c-erbB-2 mRNA, was higher after irradiation with UV light than after irradiation with visible light (Figure 2). After irradiation, the RNA cleavage reaction mixtures were incubated in the dark at 37 °C. The reaction was carried out under multiple-turnover conditions with the concentration of RNA substrate 10 times higher than that of Rb8X in the mixture. After 30 min, 38% of c-erbB-2 mRNA was digested by the Rb8X irradiated with UV light (Figure 2A), while ribozyme irradiated with visible light (Vis) cleaved almost none of the substrate. After 2 h, 88% of substrate was cleaved by the ribozyme irradiated with UV light, and only 9% was cleaved by the ribozyme irradiated with visible light. Therefore, efficient photoregulation of RNA cleavage was achieved presumably by controlling the topological structure of the ribozyme via the covalently linked supraphotoswitch. We also engineered another photoresponsive ribozyme, which was regulated by the hybridization of azobenzene-modified sequences to the catalytic loop, but the efficiency of photoregulation of this ribozyme was much lower (see Supporting Information Figure S1).

The reaction rates for wild-type ribozyme (wRb), *cis*-Rb8X (UV), and *trans*-Rb8X (Vis), obtained from the profiles of the RNA cleavage time course (Figure 2B), were 43.9, 18.7, and 1.77 nM/min, respectively. The ratio of the reaction rate of ribozyme irradiated with UV versus that irradiated with visible light (designated as photoregulation efficiency and abbreviated as α) was as large as 10.6 (α = 10.6). Interestingly, the *cis*-Rb8X (about 45% azobenzenes were in *cis* form, see Supporting Information Figure S2) had a reaction rate close to that of wRb (Figure 1b), indicating that most of the supraphotoswitch was in the open state. Photoregulation was possible in a buffer with a lower concentration of $MgCl_2$; however, the regulation efficiency was lower (Supporting Information Figure S3).

Once the *trans*-azobenzene forms a stable duplex, it is difficult to isomerize to the *cis* form (29−31). Here, the hybridization of RNA substrate to the modified ribozyme may have facilitated the isomerization of *trans* azobenzene to the *cis* form and the opening of the artificial duplex of the supraphotoswitch. Some cleavage was also observed after visible light irradiation. The slow cleavage was probably due to the partial dissociation of the supraphotoswitch. Alternatively, ribozyme dimers could form during the annealing process, although the lower concentration of the ribozymes greatly reduced the probability of this intermolecular hybridization (see Supporting Information Figure S4). For photoregulation, lower reaction temperatures and/or longer supraphotoswitch duplexes may mediate more complete photoregulation because the suppression of RNA cleavage should become more efficient under either of these conditions.

dx.doi.org/10.1021/sb300120n | *ACS Synth. Biol.* 2013, 2, 194−202

Reversibly Photoswitching of RNA Cleavage by Rb8X. One merit of this molecular design is that the supraphotoswitch can be repeatedly and reversibly turned on and off. The chemical structure of the azobenzenes is very stable in an aqueous buffer with a pH range of 6−8. Here, the real-time photoswitching Rb8X RNA-cleavage activity was performed under multiple-turnover conditions (Figure 3). Repeatedly, the reaction

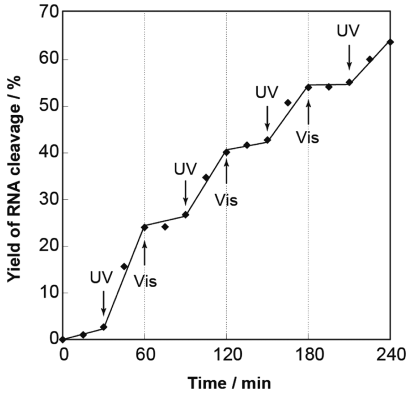

Figure 3. Photoswitching of RNA cleavage by Rb8X. The reaction mixture was alternately irradiated with UV (5 min) or visible light (1.0 min) at 37 °C. Conditions: 0.1 μM ribozyme, 1.0 μM sRb (RNA substrate), 1.0 M NaCl, 10 mM $MgCl_2$, 37 °C.

mixture was alternately irradiated with UV (5 min) or visible (1 min) light and then incubated at 37 °C for 30 min in the dark. Initially, the reaction mixture was irradiated with visible light and little RNA digestion was observed after 30 min. When the reaction system was irradiated with UV light, RNA cleavage was observed immediately (Figure 3). The reaction mixture was subjected to four rounds of photoswitching; the inhibition and activation of catalysis were completely reversible and there was no obvious deviation in photoregulation. Therefore, we concluded that this molecular design was successful, and we had achieved reversible photoregulation of hammerhead-mediated RNA cleavage.

As hammerhead ribozymes have been applied *in vivo* for suppressing gene expression by cleaving mRNA,[41] photoswitching gene expression in a cell should be possible by using a photoresponsive ribozyme. Because the azobenzene-modified strands are attached at each end of the ribozyme, the resistance to exonuclease digestion, which is an important attribute for *in vivo* applications, is expected. No degradation of Rb8X was observed after 20 h of incubation with Exonuclease T, a nuclease that digests single-stranded DNA and RNA from the 3′ end, but obvious digestion of wRb was observed after only 10 min (see Supporting Information Figure S5).

Photoswitching of RNA Digestion by Using a Photoresponsive DNAzyme. *Photoswitching of RNA Cleavage by a Photoresponsive 8−17 DNAzyme.* To investigate the versatility of our strategy for reversible photoregulation of RNA cleavage by generation and release of supraphotoswitch duplexes within functional nucleic acids, we also attached supraphotoswitches to several DNAzymes, which display higher chemical and biological stability than ribozymes.[41,42] Initially, we tested a modified 8−17 DNAzyme, which has different catalytic loop and different target site from the 10−23 DNAzyme we used previously.[42]

Figure 4A shows the structure of photoresponsive 8−17 DNAzyme (8−17Dz8X). It has a 14-nt catalytic loop, while the hammerhead ribozyme has a 20-nt catalytic loop. The same supraphotoswitch used in Rb8X was attached to 8−17Dz8X. As shown in Figure 4B, the results of photoswitching experiments demonstrate that reversible photoregulation (photoswitching) of 8−17Dz8X was realized and the strategy using a supraphotoswitch was applicable to 8−17 DNAzyme. We used a relatively lower concentration of $MgCl_2$ (2.0 mM) because the reaction rate was too fast with 10 mM $MgCl_2$ (Supporting Information Figure S6). The reaction rate of the *cis*-form of photoresponsive 8−17Dz8X (after UV light irradiation) was also a little bit slower than that of the wild-type 8−17 DNAzyme (Supporting Information Figure S6).

Photoregulation of RNA Cleavage by Photoresponsive 10−23 DNAyzmes. Previously, we have shown that photoswitching of RNA cleavage activity at GU, AU, GC, and UU sites could be carried out with a photoresponsive 10−23 DNAzyme (10−23Dzb7X).[28,43] In that case, the binding arms that had the similar sequences were used. As shown in Figure 5A, the two binding arms are partially complementary and can hybridize with each other so that the RNA substrate was hard to bind. To investigate the versatility of our strategy, we synthesized two additional photoresponsive 10−23 DNAzymes

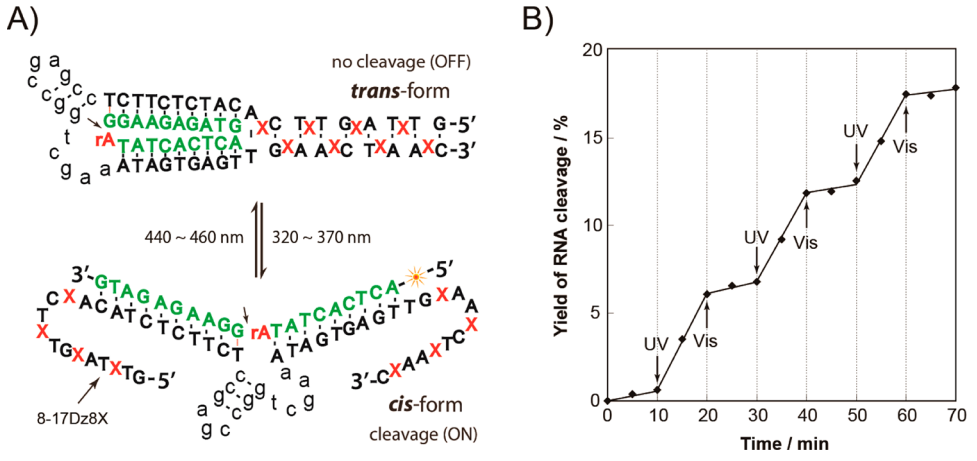

Figure 4. Molecular design of a photoresponsive 8−17 DNAzyme (A) and the results of photoswitching experiment (B). Reaction conditions: 0.1 μM 8−17Dz8X, 1.0 μM s8−17Dz (RNA substrate), 100 mM NaCl, 2.0 mM $MgCl_2$, 37 °C. The reaction mixture was alternately irradiated with UV (5 min) or visible light (1 min) at 37 °C.

dx.doi.org/10.1021/sb300120n | *ACS Synth. Biol.* 2013, 2, 194−202

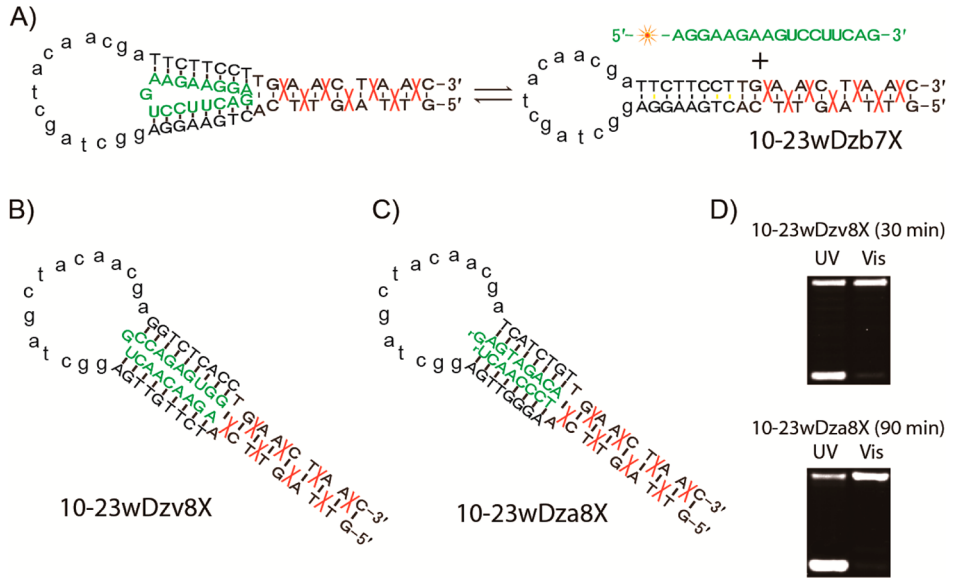

Figure 5. Structures and activity of photoresponsive 10−23 DNAzymes. (A) 10−23Dzb7X, (B) 10−23Dzv8X, and (C) 10−23Dza8X are shown in the closed state. (D) Photoregulation of RNA cleavage by 10−23Dzv8X and 10−23Dza8X. In (A), the secondary structure formed between the substrate binding arms is also shown. Reaction conditions for the digests shown in (D): 0.1 μM 10−23Dzv8X, 1.0 μM s10−23Dzv (RNA substrate), 1.0 M NaCl, 2.0 mM $MgCl_2$, 37 °C; 0.1 μM 10−23Dza8X, 1.0 μM s10−23Dza (RNA substrate), 1.0 M NaCl, 10 mM $MgCl_2$, 37 °C.

that targeted different RNA substrates (Figure 5B,C). The DNAzyme 10−23Dzv8X targeted VR1, the mRNA encoding the vanilloid receptor 1B;[44−46] and the other DNAzyme, 10−23Dza8X, targeted Asp2, the mRNA encoding aspartyl protease.[47] No stable secondary structure can form between the substrate binding arms of 10−23Dzv8X, but several fully matched base pairs can form between the substrate binding arms of 10−23Dza8X (Supporting Information Figure S7). As shown in Figure 5D, efficient photoregulation was also obtained with both catalysts. The photoregulation efficiency (α) of 10−23Dzv8X and 10−23Dza8X was 10.1 and 17.7, respectively. Thus, for each functional nucleic acid tested, efficient photoregulation was possible, demonstrating that our strategy of controlling topological structure can be generally applied to functional nucleic acids that catalyze RNA cleavage.

The photoregulation efficiency, α value, of 10−23Dzb7X, the previous photoresponsive 10−23 DNAzyme we used, was as large as 38, which was much higher than the α value of either 10−23Dzv8X or 10−23Dza8X.[28] This large difference indicates that photoregulation efficiency depends on the arm sequences. The extremely high α value of 10−23Dzb7X can be explained by the inhibition of binding between RNA substrate and 10−23Dzb7X in *trans* form (Figure 5A). Actually, the difference in photoregulation efficiency between 10 and 23Dzv8X and 10−23Dza8X can also be explained by the difference in substrate/catalyst binding affinity. The substrate binding arms of 10−23Dza8X can hybridize with each other more easily than those of 10−23Dzv8X, resulting in a larger α value for 10−23Dza8X (Supporting Information Figure S7). The length of substrate/catalyst complex can also affect photoregulation efficiency. Shorter stretches of substrate/catalyst complex (10−23Dzb7X and 10−23Dza8X) facilitate efficient suppression of RNA cleavage in *trans* form due to the more difficult hybridization. It should be noted that partial hybridization between two binding arms of a ribozyme or DNAzyme can also make the modified duplex become more difficult to dissociate in *trans* form and suppress the unexpected RNA cleavage.

Mechanisms Mediating Photoswitching of RNA Cleavage Catalyzed by Photoresponsive Functional Nucleic Acids. *Two Factors Are Topologically Constrained in Trans Form Resulting in Suppression of RNA Cleavage.* There are two factors that may suppress RNA cleavage activity when the ends of the substrate binding arms are pulled together. Topological constraint may change the structure of the catalytic site, and the crowding of negative charges may inhibit the hybridization of RNA substrate to the substrate binding arms of the catalyst. Quantitative or semiquantitative analysis of the effect of these two factors is required to optimize the molecular design of supraphotoswitches for attaining more efficient photoregulation. Here, several experiments were performed to elucidate the effects of supraphotoswitches on the topology of functional nucleic acids.

Figure 6 shows the gel shift assay using sRb, an FITC-labeled RNA substrate, and unlabeled ribozyme Rb8X. The concentration of RNA was fixed at 1.0 μM, and the concentration of Rb8X was 0.1, 0.5, or 2.0 μM. Here, the azobenzenes in Rb8X was in the *trans* form, and the supraphotoswitch was in the duplex state. When 2.0 μM of Rb8X was present, all the FITC-

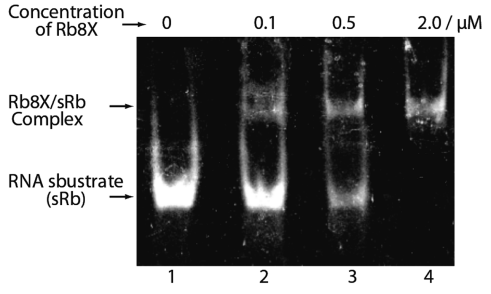

Figure 6. Gel shift assay of RNA substrate/Rb8X (*trans* form) complex formation. RNA substrate was labeled with FITC. The concentration of the RNA substrate was 1.0 μM, and the concentration of Rb8X was 0, 0.1, 0.5, or 2.0 μM. $MgCl_2$ (10 mM) was present in the gel and the electrophoresis buffer.

dx.doi.org/10.1021/sb300120n | *ACS Synth. Biol.* 2013, 2, 194−202

labeled substrate showed lower mobility (lane 4 in Figure 6). Even with 0.1 μM of Rb8X, a gel shift was also observed, indicating that the RNA substrate can bind to Rb8X even in the topologically constrained state (lane 2 in Figure 6). Thus, we concluded that the decreased in RNA cleavage activity of *trans*-Rb8X did not entirely result from an inhibition of binding of RNA substrate to the catalyst. Therefore, topological constraints on the catalytic loop should be the main factor suppressing RNA cleavage in this case.

The supraphotoswitch might open even when azobenzenes residues take the *trans* form under visible light, especially when the ion strength is low. A circular 10–23 DNAzyme was designed to assess quantitatively the effect of topological constraint on the catalytic site (Figure 7A). DNAzyme 10–23wDzv was selected because it showed very high RNA cleavage activity and relatively low photoregulatory efficiency. Notably, the substrate binding arms of 10–23wDzv cannot form a stable secondary structure that could prevent the binding of RNA substrate (Figure 7A). Circularization of 10–23wDzv was carried out according to a method described previously.[48,49] After circularization, the unreacted linear DNAzyme was digested by Exonuclease VII and then by Exonuclease T. The digestion should have been complete, and no linear DNAzyme was observed on a PAGE gel (Figure 7B).

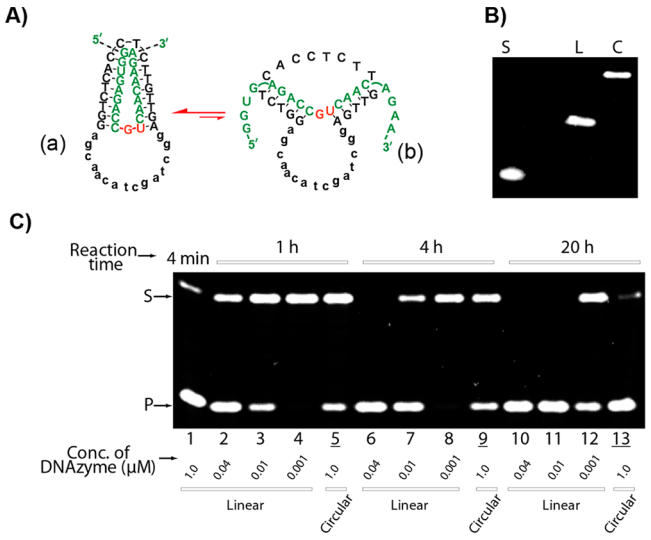

Figure 7. RNA cleavage by a circular DNAzyme. (A) Illustration of the complex of a circular DNAzyme and a RNA substrate. (B) Gel analysis of the circular DNAzyme. (C) Comparison of the RNA cleavage activity of the circular DNAzyme with that of the corresponding wild-type linear DNAzyme (10–23wDzv) at various catalyst concentrations. In (B), S, L, and C indicate RNA substrate, linear DNAzyme, and circular DNAzyme, respectively. The gel was stained with SYBR Green II. In (C), lane 1, linear 10–23wDzv and the circular DNAzyme are at the same concentration (1.0 μM), and the reaction time is 4 min; reaction mixtures in lanes 2, 6, and 10 contain linear 10–23wDzv at 0.04 μM; lanes 3, 7, and 11 contain linear 10–23wDzv at 0.01 μM; lanes 4, 8, and 12 contain linear 10–23wDzv at 0.001 μM. Lanes 5, 9, and 13 contain reaction mixtures with circular DNAzyme (1.0 μM). Reaction conditions: 1.0 μM s10–23Dzv (RNA substrate), 1.0 M NaCl, 10 mM $MgCl_2$, 37 °C.

As shown in Figure 7C, after 4 h of cleavage, 32% of RNA substrate was cleaved by the circular DNAzyme (lane 9). However, when the same concentration of linear one was used, 90% of RNA was cut in 4 min (lane 1). For the circular DNAzyme, cleavage of 90% of RNA required about 20 h (compare lane 13 with lane 1). The RNA cleavage rate in reaction mixtures containing circular DNAzyme was slower than those with only 0.01 μM of linear DNAzyme (lane 3, 7, and 11). It can be concluded that the topological constraint caused by circularization of the DNAzyme inhibited RNA cleavage by at least 100-fold; i.e., the circular DNAzyme showed less than 1% of the activity of the linear DNAzyme (compare lane 7 with lane 9). Interestingly, even when 0.001 μM of linear DNAzyme was used (lane 4, 8, and 12), RNA was also cleaved after 20 h (lane 12). When a spacer of $(dT)_n$ (n = 2, 4, 6, 8) was added to release the topological constraint, the cleavage activity was recovered gradually (data not shown). This result demonstrated clearly that the topological constraint could suppress the RNA cleavage greatly.

The left cleavage activity of the circular DNAzyme (lane 13 in Figure 7C) may be caused by a temporal and partly hybridized structure (see structure b in Figure 7A). In the case of photoresponsive ribozymes or DNAzymes, suppression of RNA cleavage when azobenzene residues take the *trans* form, which is important for efficient photoregulation, was not so large as that of the circular DNAzyme. The temporal dissociation of the supraphotoswitch duplex, which may be accelerated by either hybridization of RNA target and/or by dimerization of photoresponsive ribozyme or DNAzymes, should be the main reason for the noncomplete suppression of RNA cleavage.

Another factor that affects the photoregulated suppression of RNA cleavage is the inhibited hybridization between RNA substrate and the topologically constrained substrate binding arms. A gel shift assay of binding between an RNA substrate (s10–23Dzb7X) and a DNAzyme (10–23Dzb7X) showed that almost no DNAzyme/substrate complex formed (data not shown). The difference in photoregulation efficiency between 10 and 23Dzb7X and 10–23Dzv8X may be explained by a difference in their binding affinity to substrates when azobenzene residues take the *trans* form (Figure 5). In addition, the partial hybridization between two binding arms also strengthens the stability of the stem duplex (supraphotoswitch part) and contributes to the suppression of RNA cleavage.

Conclusions. In conclusion, we have developed a versatile strategy for controlling the activity of functional oligonucleotides that involve modulating their topological structures. This strategy can be used to efficiently photoregulate the biological activity of functional oligonucleotides that have two substrate binding arms and a catalytic loop. For those RNA-cleaving ribozymes and DNAzymes investigated in this study, the regulated inhibition of RNA cleavage was attributed to conformation constraints at the catalytic loop and suppression of substrate/catalyst binding caused by the duplex that forms when azobenzene residues take the *trans* form. The inhibited activity for the visible-irradiated enzymes is mainly due to the slower catalysis of topologically constrained structure, although the decrease of substrate binding helps to improve the regulation efficiency in some cases. If we can design a system in which the two factors are combined, a clear-cut regulation can be obtained. Longer supraphotoswitches, shorter substrate binding arms, selection of cleavage target resulting in appropriate secondary structure formed between two arms, and lower concentrations of the photoresponsive catalyst should favor more complete and precise photoinduced suppression of activity. However, it should be noted that very long supraphotoswitch duplexes may prevent smooth dissoci-

dx.doi.org/10.1021/sb300120n | *ACS Synth. Biol.* 2013, 2, 194–202

Table 1. DNA and RNA Sequences Used in This Study[a]

sRb	5′-FITC-AUCAAAGUGUU↓GAGGGAAA-3′
wRb	5′-5Phos/UUUCCCUCCUGAUGAGUCGUGAGACGAAACACUUUGAU-3′
Rb8X	5′-GTXTAXGTXTCXAUUUCCCUCCUGAUGAGUCGUGAGACGAAACACUUUGAUTGXAAXCTXAAXC-3′
Rb4X	5′-GAXCTXCAXTCXAUUUCCCUCCUGAUGAGUCGUGAGACGAAACACUUUGAU-3′
s8−17Dz	5′-FITC-ACTCACTAT rA↓GGAAGAGATG-3′
8−17wDz	5′-CATCTCTTCTCCGAGCCGGTCGAAATAGTGAGT-3′
8−17Dz8X	5′-GTXTAXGTXTCXACATCTCTTCTCCGAGCCGGTCGAAATAGTGAGTTGXAAXCTXAAXC-3′
s10−23Dzv	5′-FITC-GGUGAGACCG↓UCAACAAGA-3′
10−23wDzv	5′-AGG GTT GA GGC TAG CTA CAA CGA TCA TCT GT-3′
10−23Dzv8X	5′-GTXTAXGTXTCXATCTTGTTGAGGCTAGCTACAACGAGGTCTCACCTGXAAXCTXAAXC-3′
s10−23Dza	5′-FITC-ACAGATGArG↓rUCAACCCT-3′
10−23wDza	5′-AGGGTTGAGGCTAGCTACAACGATCATCTGT-3′
10−23Dza8X	5′-GTXTAXGTXTCXAAGGGTTGAGGCTAGCTACAACGATCATCTGTTGXAAXCTXAAXC-3′
s10−23Dzb	5′-FITC-AGGAAGAAG↓UCCUUCAG-3′
10−23wDzb	5′-CTGAAGGAGGCTAGCTACAACGATTCTTCCT-3′
10−23Dzb7X	5′-GTXTAXGTXTCACTGAAGGAGGCTAGCTACAACGATTCTTCCTTGXAAXCTXAAXC-3′
10−23wDzv-L	5′-AACAAGAGGTGAGA-3′

[a]X indicates the azobenzene residue. In the substrate s8-17Dz and s10-23Dza, only one (rA) or two nucleotides (rG and rU) at the cleavage site are RNA nucleotides, and the left ones are deoxyribonucleotides. The arrow in the substrate sequence indicates the cleavage site.

ation of two strands even under UV light irradiation due to the relative difficulty of isomerizing to the *cis* form. Optimization of the length and the complementarity of substrate binding arms can enhance the topological constraint.[49,50]

The above analyses of the mechanisms of photoregulation can help us to design photoresponsive oligonucleotides for actual applications in photoregulation of gene expression in cells. When actual, long mRNA is targeted, improvements in photoregulation efficiency can be expected because the hybridization with the topologically constrained substrate binding arms becomes more difficult. The long mRNA must hybridize with two closed arms to form a double helix structure. Although photoregulation of RNA cleavage activity of 8−17 DNAzyme and 10−23 DNAzyme has also been reported by other groups by introducing azobenzenes to the catalytic core or binding arms, there should be no topological constraint for cleaving long mRNA in these cases.[51,52] The left cleavage activity in *trans* form may cause problems to limit the applications. Both the molecular design to reduce this background cleavage and the adjustment of proper concentration of modified enzymes in cells should be considered. It is also a challenge when reversible photoregulation is carried out in cells. In addition, the longer wavelength of UV light (>365 nm) should be used to reduce the damage of cell by UV light. The cells should be covered during UV sterilization to avoid unexpected photoisomerization. The application of our strategy on photoswitching gene expression *in vivo* by targeting mRNA is currently underway.

METHODS

Oligonucleotides and Reagents. Oligonucleotides containing only natural bases (ribozyme, DNAzyme, RNA substrates labeled with FITC (Fluorescein Isothiocyanate), and short DNA for circularization of DNAzyme) were prepared by automated DNA/RNA synthesis using standard phosphoramidite chemistry and purified by either polyacrylamide gel electrophoresis or HPLC (Integrated DNA Technologies, Coralville, IA, USA). Oligonucleotides containing azobenzene residues were supplied by Nihon Techno Service Co., Ltd. (Tsukuba, Japan), and purified by polyacrylamide gel electrophoresis. The concentration of all oligonucleotides was determined by UV−vis spectroscopic within a 10% margin of error. All DNA and RNA sequences used in this study are listed in Table 1. Exonuclease T was purchased from NEB (New England Biolabs, Ipswich, MA, USA). Exonuclease VII was purchased from EPICENTRE Biotechnologies (Madison, WI, USA). T4 DNA ligase was purchased from Invitrogen Life Technologies (Madison, WI, USA).

RNA Cleavage by Ribozyme or DNAzyme. A typical ribozyme- or DNAzyme-catalyzed RNA cleavage reaction was performed as follows.[28] Substrate RNA and the catalyst (ribozyme or DNAzyme) were mixed with buffer (e.g., 1.0 M NaCl, 50 mM Tris-HCl, pH 7.5) in a final volume of 20 μL; the mixture was heated to 90 °C for 1.0 min. The mixture was cooled to 37 °C over 30 min to allow for annealing between the substrate and the catalyst; the mixture was then irradiated with visible light (440−460 nm, 90 mW cm^{-2}, 1.0 min) or UV light (320−370 nm, 5.3 mW cm^{-2}, 5 min) by using a Xenon light source (MAX-301, Asahi Spectra Co., Ltd. Tokyo, Japan) and allowed to reach a photoequilibrium state. $MgCl_2$ was added to a certain concentration, e.g., 10 mM, to start the cleavage reaction at 37 °C. After a set time interval, 4.0 μL of the mixture was added to 4.0 μL of 2× loading buffer (50 mM EDTA, 45 mM Tris-HCl, 45 mM borate, 7.0 M urea) to terminate the reaction. The resulting mixture (8.0 μL) was subjected to electrophoresis on a 20% denaturing polyacrylamide gel containing 7.0 M urea. Imaging and quantification of the digested RNA were carried out on a Fujifilm FLA-3000G fluorescent analyzer (Fuji Film, Tokyo, Japan). The fluorescence of FITC (excitation 473 nm, emission 520 nm), which was attached to 5′-end of RNA substrate (Table 1), was detected. For real-time photoswitching of RNA digestion, UV and visible light were applied alternatively after the $MgCl_2$ was added.

Gel Shift Assay. The gel shift assay of sRb binding on ribozyme Rb8X was carried out as follows. A mixture of 5′-labeled sRb and Rb8X (*trans* form) in 1× reaction buffer (1.0 M NaCl, 50 mM Tris-HCl, pH 7.5) without $MgCl_2$ was heated to 90 °C and held there for 1.0 min; the mixture was then slowly cooled to 37 °C over 30 min. The concentration of sRb was fixed at 1.0 μM, and the concentration of Rb8X was adjusted to 0, 0.1, 0.5, or 2.0 μM. $MgCl_2$ (10 mM) and 2×

dx.doi.org/10.1021/sb300120n | *ACS Synth. Biol.* 2013, 2, 194−202

loading buffer (2.0 mM Tris-HCl (pH 7.5), 0.06 (w/v) % BPB and Xylene cyanol, 10 (v/v) % glycerine) was then added, and the mixture was immediately loaded onto a native PAGE and subjected to electrophoresis. 10 mM $MgCl_2$ was also present in the running buffer (1 × TBE). The temperature of electrophoresis apparatus was kept at 15−20 °C during the electrophoresis for 40 min. Imaging was carried out with the same method as described for the assay of RNA cleavage.

Circularization of DNAzyme (10−23wDzv). Lyophilized 5′-phosphorylated 10−23wDzv was resuspended in 100 μL of 1× ligation buffer (40 mM Tris-HCl (pH 7.8 at 25 °C), 10 mM $MgCl_2$, 10 mM DTT, 0.5 mM ATP) with a short DNA wDzv-L as the splint. The final concentrations of 10−23wDzv and wDzv-L were 1.0 and 2.0 μM, respectively. The mixture was heated to 80 °C and held for 1.0 min and then cooled slowly (about 2 °C/min) to 25 °C. T4 DNA ligase (5 units) was then added to the mixture, which was then incubated at 25 °C for 2.0 h, and the ligase was then inactivated by heating to 65 °C for 15 min. The T4 DNA ligase was extracted with PCI (phenol/chloroform/isoamylalcohol = 25:24:1) and CIA (chloroform/isoamylalcohol = 24:1), and the circular DNA product was precipitated in ethanol and dissolved in sterile water. Linear single-stranded 10−23wDzv and splint DNA (10−23wDzv-L) were digested by Exonuclease VII for 30 min in the standard reaction buffer (50 mM Tris-HCl (pH 7.9), 50 mM sodium phosphate (pH 7.8), 10 mM 2-mercaptoethanol, and 8.4 mM EDTA). Finally, the DNA product was digested with Exnuclease T in the following conditions (in 20 μL): 5.0 μM DNA product, 1.5 U Exonuclease T, incubated at 25 °C for 2.0 h in 1× NEBuffer 4 (20 mM Tris-acetate, 50 mM potassium acetate (pH 7.9 at 25 °C), 10 mM magnesium acetate, 1.0 mM dithiothreitol). After digestion, the mixture was heated to 65 °C and held for 20 min to inactivate Exonuclease T. The circular 10−23wDzv was purified by PCI (phenol/chloroform/isoamylalcohol = 25:24:1) and CIA (chloroform/isoamylalcohol = 24:1) treatment and ethanol precipitation. The cleavage of RNA by the prepared circular DNAzyme was carried out according to the procedure as described in the RNA cleavage section.

Digestion of Photoresponsive Ribozyme by Exonuclease T. Wild-type hammerhead ribozyme (wRb), photoresponsive ribozyme (Rb8X) and their substrate RNA (sRb) were digested with Exonuclease T in a 20-μL reaction volume under the following conditions: 1.0 μM RNA, 5.0 U Exonuclease T, incubated at 25 °C for 20 h in 1× NEBuffer 4 (20 mM Tris-acetate, 50 mM potassium acetate (pH 7.9 at 25 °C), 10 mM magnesium acetate, 1.0 mM dithiothreitol). After digestion, the mixture was heated to 65 °C and held for 20 min to inactivate Exonuclease T. Digestion products were sampled at 0, 5, 30 min, and 20 h and were then analyzed on a 20% denaturing polyacrylamide gel containing 7.0 M urea.

■ ASSOCIATED CONTENT

Ⓢ Supporting Information

Supporting experiment results are shown in Figures S1−S6: Photoresponsive ribozyme with only one modified arm (Figure S1), photoisomerization of azobenzenes in Rb8X (Figure S2), cleavage at lower concentration of $MgCl_2$ (Figure S3), possible dimer structure of Rb8X (Figure S4), digestion of Rb8X by Exonuclease T (Figure S5), cleavage by 8−17Dz8X under other conditions (Figure S6). Figure S7 shows the secondary structure of 10−23Dza8X. This material is available free of charge via the Internet at http://pubs.acs.org.

■ AUTHOR INFORMATION

Corresponding Author

*Tel: (+86) 532-8203-1086. Fax: (+81) 52-789- 2528. E-mail: liangxg@ouc.edu.cn; asanuma@nubio.nagoya-u.ac.jp.

Author Contributions

Xingguo Liang designed the experiments and wrote the paper. Mengguang Zhou did most of the experiments. Kenjiro Kato did some of the experiments. Hiroyuki Asanuma discussed the results, gave suggestions, and reviewed the manuscript. The manuscript was written through contributions of all authors. All authors have given approval to the final version of the manuscript.

Notes

The authors declare no competing financial interest.

■ ACKNOWLEDGMENTS

This work was supported by two Grants-in-Aid for Scientific Research [No. 20750132, 21241031] and Grant-in-Aid for Scientific Research on Innovative Areas "Molecular Robotics" [No. 24104005] from the Ministry of Education, Culture, Sports, Science and Technology, Japan. The Tatematsu Foundation, Shandong Provincial Natural Science Foundation [No.201204], and Program for Changjiang Scholars and Innovative Research Team in Ocean University of China from Ministry of Education of China provided support to X.L., and G-COE Nagoya University provided support to M.Z.

■ ABBREVIATIONS

DNAzyme, DNA enzyme; ALS, amyotrophic lateral sclerosis; FITC, Fluorescein isothiocyanate

■ REFERENCES

(1) Mayer, G., and Heckel, A. (2006) Biologically active molecules with a 'light switch'. *Angew. Chem., Int. Ed. 45*, 4900−4921.

(2) Deiters, A. (2009) Light activation as a method of regulating and studying gene expression. *Curr. Opin. Chem. Biol. 13*, 678−686.

(3) Chou, C., Young, D. D., and Deiters, A. (2009) A light-activated DNA polymerase. *Angew. Chem., Int. Ed. 48*, 5950−5953.

(4) Young, D. D., and Deiters, A. (2007) Photochemical control of biological processes. *Org. Biomol. Chem. 5*, 999−1005.

(5) Tang, X., and Dmochowski, I. J. (2007) Regulating gene expression with light-activated oligonucleotides. *Mol. BioSyst. 3*, 100−110.

(6) Lewandoski, M. (2001) Conditional control of gene expression in the mouse. *Nat. Rev. Genet. 2*, 743−755.

(7) Ando, H., Furuta, T., Tsien, R. Y., and Okamoto, H. (2001) Photo-mediated gene activation using caged RNA/DNA in zebrafish embryos. *Nat. Genet. 28*, 317−325.

(8) Shah, S., Rangarajan, S., and Friedman, S. H. (2005) Light-activated RNA interference. *Angew. Chem., Int. Ed. 44*, 1328−1332.

(9) Link, K. H., Shi, Y., and Koh, J. T. (2005) Light activated recombination. *J. Am. Chem. Soc. 127*, 13088−13089.

(10) Volgraf, M., Gorostiza, P., Numano, R., Kramer, R. H. E., Isacoff, Y., and Trauner, D. (2006) Allosteric control of an ionotropic glutamate receptor with an optical switch. *Nat. Chem. Biol. 2*, 47−52.

(11) Shah, S., Rangarajan, S., and Friedman, S. H. (2005) Light-activated RNA interference. *Angew. Chem., Int. Ed. 44*, 1328−1332.

(12) Shimizu, S., Huq, E., Tepperman, J. M., and Quail, P. H. (2002) A light-switchable gene promoter system. *Nat. Biotechnol. 20*, 1041−1044.

(13) Asanuma, H., Liang, X. G., Nishioka, H., Matsunaga, D., Liu, M., and Komiyama, M. (2007) Synthesis of azobenzene-tethered DNA for reversible photo-regulation of DNA. *Nat. Protoc. 2*, 203−212.

(14) Levskaya, A., Chevalier, A. A., Tabor, J. J., Simpson, Z. B., Lavery, L. A., Levy, M., Davidson, E. A., Scouras, A., Ellington, A. D.,

Marcotte, E. M., and Voigt, C. A. (2005) Engineering *Escherischia coli* to see light. *Nature 438*, 441−442.
(15) Cruz, F. G., Koh, J. T., and Link, K. H. (2000) Light-activated gene expression. *J. Am. Chem. Soc. 122*, 8777−8778.
(16) Ando, H., Furuta, T., and Okamoto, H. (2004) Photo-mediated gene activation by using caged mRNA in zebrafish embryos. *Methods Cell. Biol. 77*, 159−171.
(17) Pinheiro, A. V., Baptista, P., and Lima, J. C. (2008) Light activation of transcription: photocaging of nucleotides for control over RNA polymerization. *Nucleic Acids Res. 36*, e90.
(18) Monroe, W. T., McQuain, M. M., Chang, M. S., Alexander, J. S., and Haselton, F. R. (1999) Targeting expression with light using caged DNA. *J. Biol. Chem. 274*, 20859−20900.
(19) Jayapal, P., Mayer, G., Heckel, A., and Wennmohs, F. (2009) Structure−activity relationships of a caged thrombin binding DNA aptamer: Insight gained from molecular dynamics simulation studies. *J. Struct. Biol. 166*, 241−250.
(20) Mikat, V., and Heckel, A. (2007) Light-dependent RNA interference with nucleobase-caged siRNAs. *RNA 13*, 2341−2347.
(21) Heckel, A., and Mayer, G. (2005) Light regulation of aptamer activity: An anti-thrombin aptamer with caged thymidine nucleobases. *J. Am. Chem. Soc. 127*, 822−823.
(22) Flint, D. G., Kumita, J. R., Smart, O. S., and Woolley, G. A. (2002) Using an azobenzene cross-linker to either increase or decrease peptide helix content upon trans-to-cis photoisomerization. *Chem. Biol. 9*, 391−397.
(23) Liu, D., Karanicolas, J., Yu, C., Zhang, Z., and Woolley, G. A. (1997) Site-specific incorporation of photoisomerizable azobenzene groups into ribonuclease S. *Bioorg. Med. Chem. Lett. 7*, 2677−2680.
(24) Behrendt, R., Renner, C., Schenk, M., Wang, F., Wachtveitl, J., Oesterhelt, D., and Moroder, L. (1999) Photomodulation of the conformation of cyclic peptides with azobenzene moieties in the peptide backbone. *Angew. Chem., Int. Ed. 38*, 2771−2774.
(25) Loweneck, M., Milbradt, A. G., Root, C., Satzger, H., Zinth, W., Moroder, L., and Renner, C. (2006) A conformational two-state peptide model system containing an ultrafast but soft light switch. *Biophys. J. 90*, 2099−2108.
(26) Liang, X. G., Wakuda, R., Fujioka, K., and Asanuma, H. (2010) Photo-regulation of DNA transcription by using photo-responsive T7 promoters and clarification of its mechanism. *FEBS J. 277*, 1551−1561.
(27) Liu, M. Z., Asanuma, H., and Komiyama, M. (2006) Azobenzene-tethered T7 promoter for efficient photo-regulation of transcription. *J. Am. Chem. Soc. 128*, 1009−1015.
(28) Zhou, M. G., Liang, X. G., Mochizuki, T., and Asanuma, H. (2010) A light-driven DNA nanomachine for the efficient photo-switching of RNA digestion. *Angew. Chem., Int. Ed. 49*, 2167−2170.
(29) Liang, X. G., Mochizuki, T., and Asanuma, H. (2009) A supra-photoswitch involving sandwiched DNA base pairs and azobenzenes for light-driven nanostructures and nanodevices. *Small 5*, 1761−1768.
(30) Liang, X. G., Nishioka, H., Mochizuki, T., and Asanuma, H. (2010) An interstrand-wedged duplex composed of alternating DNA base pairs and covalently attached intercalators. *J. Mater. Chem. 20*, 575−581.
(31) Liang, X. G., Mochizuki, T., Fujii, T., Kashida, H., and Asanuma, H. (2011) Design of a functional nanomaterial with recognition ability for constructing light-driven nanodevices. *Lect. Notes Comput. Sci. 6518*, 112−122.
(32) Tanaka, F., Mochizuki, T., Liang, X. G., Asanuma, H., Tanaka, S., Suzuki, K., Kitamura, S., Nishikawa, A., Ui-Tei, K., and Hagiya, M. (2010) Robust and photo-controllable DNA capsules using azobenzenes. *Nano Lett. 10*, 3560−3565.
(33) Prody, G. A., Bakos, J. T., Buzayan, J. M., Schneider, I. R., and Bruening, G. (1986) Autolytic processing of dimeric plant virus satellite RNA. *Science 231*, 1577−1580.
(34) Hutchins, C. J., Rathjen, P. D., Forster, A. C., and Symons, R. H. (1986) Self-cleavage of plus and minus RNA transcripts of avocado sunblotch viroid. *Nucleic Acids Res. 14*, 3627−3640.
(35) Citti, L., and Rainaldi, G. (2005) Synthetic hammerhead ribozymes as therapeutic tools to control disease genes. *Curr. Gene Ther. 5*, 11−24.
(36) Hean, J., and Weinberg, M. S. (2008) The hammerhead ribozyme revisited: New biological insights for the development of therapeutic agents and for reverse genomics applications. *Rna and the Regulation of Gene Expression: A Hidden Layer of Complexity* (Morris, K. V., Ed.) Chapter 1, pp 1−18, Caister Academic Press, La Jolla, CA.
(37) Aida, T., and Jiang, D.-L. (2000) Dendrimer porphyrins and metalloporphyrins: syntheses, structures and functions. *The Porphyrin Handbook* (Kadish, K. M., Smith, K. M., and Guilard, R., Eds.) Vol. 3, Chapter 23, pp 369−384, Academic Press, New York.
(38) Martick, M., and Scott, W. G. (2006) Tertiary contacts distant from the active site prime a ribozyme for catalysis. *Cell 126*, 309−320.
(39) Bohkman, J. V. (1983) Two pathogenetic types of endometrial carcinoma. *Gynecol. Oncol. 15*, 10−17.
(40) Rio, M. C. J, Bellocq, P., Gairard, B., Rasmussen, U. B., Krust, A., Koehl, C., Calderoli, H., Schiff, V., Renaud, R., and Chambon, P. (1987) Specific expression of the pS2 gene in subclasses of breast cancers in comparison with expression of the estrogen and progesterone receptors and the oncogene ERBB2. *Proc. Natl. Acad. Sci. U. S. A. 84*, 9243−9247.
(41) Semba, K., Kamata, N., Toyoshima, K., and Yamamoto, T. (1985) A v-erbB-related protooncogene, c-erbB-2, is distinct from the c-erbB-1/epidermal growth factor-receptor gene and is amplified in a human salivary gland adenocarcinoma. *Proc. Natl. Acad. Sci. U. S. A. 82*, 6497−6501.
(42) Joyce, G. F. (2004) Directed evolution of nucleic acid enzymes. *Annu. Rev. Biochem. 73*, 791−836.
(43) Santoro, S. W., and Joyce, G. F. (1997) Mechanism and utility of an RNA-cleaving DNA enzyme. *Proc. Natl. Acad. Sci. U. S. A. 94*, 4262−4266.
(44) Kim, H. K., Li, J., Nagraj, N., and Lu, Y. (2008) Probing metal binding in the 8−17 DNAzyme by TbIII luminescence spectroscopy. *Chem.—Eur. J. 14*, 8696−8703.
(45) Szallasi, A., and Blumberg, P. M. (1999) Vanilloid (capsaicin) receptors and mechanisms. *Pharmacol. Res. 51*, 159−211.
(46) Mezey, E., Toth, Z. E., Cortright, D. N., Arzubi, M. K., Krause, J. E., Elde, R., Guo, A., Blumberg, P. M., and Szallasi, A. (2000) Distribution of mRNA for vanilloid receptor subtype 1 (VR1), and VR1-like immunoreactivity, in the central nervous system of the rat and human. *Proc. Natl. Acad. Sci. U. S. A. 97*, 3655−3660.
(47) Guo, A., Vulchanova, L., Wang, J., Li, X., and Elde, R. (1999) Immunocytochemical localization of the vanilloid receptor 1 (VR1): Relationship to neuropeptides, the P2X3 purinoceptor and IB4 binding sites. *Eur. J. Neurosci. 11*, 946−958.
(48) Hussain, I., Powell, D., Howlett, D. R., Tew, D. G., Meek, T. D., Chapman, C., Gloger, I. S., Murphy, K. E., Southan, C. D., Ryan, D. M., Smith, T. S., Simmons, D. L., Walsh, F. S., Dingwall, C., and Christie, G. (1999) Identification of a novel aspartic protease (Asp 2) as beta-secretase. *Mol. Cell. Neurosci. 14*, 419−427.
(49) Liang, X. G., Kuhn, H., and Frank-Kamenetskii, M. D. (2006) Monitoring single-stranded DNA secondary structure formation by determining the topological state of DNA catenanes. *Biophys. J. 90*, 2877−2889.
(50) Bucka, A., and Stasiak, A. (2002) Construction and electrophoretic migration of single-stranded DNA knots and catenanes. *Nucleic Acids Res. 30*, e24.
(51) Liu, Y., and Sen, D. (2004) Light-regulated catalysis by an RNA-cleaving deoxyribozyme. *J. Mol. Biol. 341*, 887−892.
(52) Keiper, S., and Vyle, J. S. (2006) Reversible photocontrol of deoxyribozyme-catalyzed RNA cleavage under multiple-turnover conditions. *Angew. Chem., Int. Ed. 45*, 3306−3309.